PHYSICAL REVIEW B **84**, 020408(R) (2011)

Pressure-induced change in the magnetic ordering of $TbMnO_3$

O. L. Makarova,[1,2] I. Mirebeau,[1,*] S. E. Kichanov,[3] J. Rodriguez-Carvajal,[4] and A. Forget[5]
[1]*CEA, Centre de Saclay, /DSM/IRAMIS/ Laboratoire Léon Brillouin, F-91191 Gif-sur-Yvette, France*
[2]*National Research Center "Kurchatov Institute," 123182 Moscow, Russia*
[3]*Frank Laboratory of Neutron Physics, JINR, 141980 Dubna, Russia*
[4]*Institut Laue-Langevin, Diffraction Group, BP 156, F-38042 Grenoble Cedex 9, France*
[5]*CEA, Centre de Saclay, /DSM/IRAMIS/ Service de Physique de l'Etat Condensé, F-91191 Gif-Sur-Yvette, France*
(Received 29 April 2011; revised manuscript received 20 June 2011; published 20 July 2011)

We have studied $TbMnO_3$ by high-pressure neutron diffraction up to 3.6 GPa and down to 1.5 K. The incommensurate spin structures of the Mn and Tb moments are strongly suppressed under pressure, and an *E*-type commensurate spin structure with $(0,1/2,0)$ propagation vector is stabilized for the Mn moments. The Mn and Tb incommensurate orders which persist at low pressures or low temperatures are also affected, with a change of phase of the modulation between neighboring Mn chains and a reorientation of the Mn moments along the *a* axis. The results suggest both a change of the balance of the different Mn-Mn interactions and a strengthening of the Tb-Tb (or Tb-Mn) interactions under pressure.

DOI: 10.1103/PhysRevB.84.020408 PACS number(s): 75.85.+t, 61.05.fm, 75.25.−j, 75.30.Kz

$TbMnO_3$ is one of the best studied multiferroics, where the cycloidal magnetic order is accompanied with a lattice modulation and the occurrence of ferroelectric polarization at the magnetic ordering temperature.[1] The main ingredients for this effect are spin frustration, leading to a complex magnetic order breaking the inversion symmetry,[2] and a strong magnetoelastic coupling, which shifts the position of the magnetic ions and provides a dipolar moment through spin-orbit and Dzyaloshinski-Moriya (DM) interactions.[3,4] This coupling allows the control of the ferrolectric polarization by a magnetic field and the observation of hybrid spin-lattice excitations.[1,5]

Many studies the magnetic structure of $TbMnO_3$ in zero and applied field,[6,7] but not under applied pressure. Pressure changes interatomic distances and therefore influences the frustration by changing the delicate energy balance of magnetic interactions which depend on these distances in different ways. In YMn_2O_5, this seems to explain the pressure-induced change of the electric polarization.[8]

Neutron diffraction under high pressure is the most direct way to determine the pressure-induced changes of a magnetic structure. It is, however, difficult due to the small sample size and low signal-to-background ratio. Moreover, in $TbMnO_3$ the neutron-diffraction patterns are intricate due to the presence of complex magnetic structures with simultaneous contributions of Tb and Mn magnetic moments. We have used cold neutrons to determine the magnetic order in a large pressure and temperature range (0–3.6 GPa; 1.5–50 K). We show that commensurate magnetic structures are stabilized at high pressures. Incommensurate structures persist at low pressures and temperatures, but they change strongly with respect to ambient pressure yielding information on the relative strength of magnetic interactions.

Powder neutron-diffraction (PND) patterns were recorded on the G6.1 diffractometer at Orphée reactor, equipped with focusing devices in the high-pressure version,[9] and using an incident neutron beam of 4.74 Å wavelength. A sample of 30 mg was mixed with a pressure transmitting medium (NaCl 40% volume), yielding a uniaxial component of ∼0.2 GPa along the pressure cell axis. The cell was inserted in a helium cryostat and the patterns recorded at pressures of 0.9, 1.3, 3.2, and 3.6 GPa for temperatures between 50 and 1.5 K. A symmetry analysis was performed in the space group *Pbnm* and the patterns were refined using the FULLPROF Suite.[10] Typical PND patterns at ambient pressure are shown in Fig. 1(a).

Below the Néel temperature ($T_N = 43$ K), the sinusoidal-wave-type ordering of the Mn^{3+} moments along the *b* axis [Fig. 1(c)] was refined as the $(0\ A_y\ 0)$ mode of the irreducible representation (IR) Γ_3 with a propagation vector $(0,k_1,0)$ ($k_1 \sim 0.27$). We use the Kovalev and Bertaut notations as in Ref. 11 (see Table I). Magnetic structures described by $\Gamma_3(0\ A_y\ 0)$ and $\Gamma_3(G_x\ 0\ 0)$ modes are called A_y and G_x for simplicity. Upon cooling below 28 K, magnetic Bragg peaks with a propagation vector $(0,3k_1,0)$ show that the modulation becomes steplike. These high-order reflections were neglected in the analysis. Below 28 K, the Mn^{3+} moments rotate over a cycloid described by combining the two modes G_x and A_y of Γ_3 defined in Table I, with moment components along *a* and *b*, respectively, in a two-dimensional modulation referred to below as (G_xA_y0). Below 8(1) K, the diffuse scattering between the Bragg peaks becomes strongly modulated, due to the ordering of the Tb^{3+} moments over a short-range length scale. The broad magnetic peaks due to Tb^{3+} moments are indexed with the propagation vector $(0,k_2,0)$, with $k_2 = 0.435$. The anisotropic peak broadening was modeled using spherical harmonics, yielding at 1.5 K typical length scales between 60 Å (along *b*) and 16 Å (along *c*). Below 8 K a good refinement was obtained assuming that both Tb^{3+} and Mn^{3+} moments describe a cycloid in the *ab* plane, described by the (G_xA_y0) mode of Γ_3.

Although a cycloid in the *bc* plane is usually assumed,[6,7] it could not account for the Tb order at low temperature. Besides this specific point, the above description is consistent with that inferred from single-crystal data. Especially, the *T* dependence of the propagation vector, the transition temperatures and the moment values [Fig. 1(b)] agree with previous observations. This description was used as a

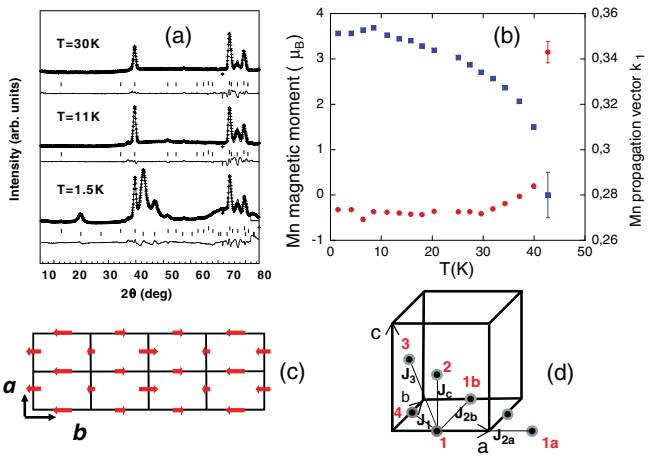

FIG. 1. (Color online) (a) Powder neutron-diffraction patterns of $TbMnO_3$ at ambient pressure. Solid lines are fits as described in the text. (b) Temperature dependence of the Mn^{3+} magnetic moment (blue squares) and k_1 propagation vector (red dots) at ambient pressure. (c) Sinusoidal wave-type ordering of the Mn moments described by the A_y mode. (d) Mn interaction scheme situating the superexchange interactions J_c and J_1 and the super-superexchange interactions J_{2b}, J_{2a}, and J_3 via two oxygen ions. Mn ions (1–4) are numbered as in Table I. Sites 1a and 1b result from lattice translations.

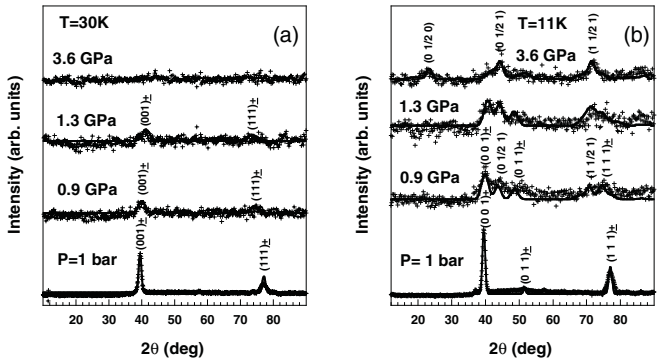

FIG. 2. $TbMnO_3$. Pressure evolution of the magnetic diffraction patterns at 30 K (a) and 11 K (b). A pattern at 50 K was subtracted. Solid lines are refinements as described in the text.

reference to analyze the effect of pressure on the magnetic order.

Under pressure drastic changes are observed in the magnetic order. They were analyzed by considering the magnetic patterns obtained by subtracting a paramagnetic pattern at 50 K. The patterns at 50 K show nuclear peaks with the same relative intensities as at ambient pressure, so we kept the same description of the crystal structure.

We first show the effect of pressure at two temperatures: 30 K where the Tb magnetism can be neglected, and 11 K, where it starts to play a role under pressure. Magnetic patterns measured at different pressures were scaled to the integrated intensity of the (110) nuclear peak to be easily compared. At 30 K [Fig. 1(a)], the incommensurate magnetic peaks associated with the sinusoidal modulation of the Mn moments become strongly diminished under pressure, and they disappear at 3.6 GPa. As no other magnetic peaks are observed, it means that the Néel temperature decreases under pressure.

At 11 K [Fig. 1(b)], other features are observed. At low pressures, the relative intensities of the k_1 satellites $(001)^{\pm}$ and $(011)^{\pm}$ associated with the incommensurate modulation of the Mn moments strongly change (Fig. 2). This corresponds to a destabilization of the A_y mode in favor of the G_x one, since in the A_y mode both $(001)^{\pm}$ and $(011)^{\pm}$ satellites are present, whereas in the G_x mode only $(011)^{\pm}$ is observed. From Table I, the change from A_y to G_x observed at low pressures reflects a dephasing of the modulations between two neighboring chains along the b axis, which reverses the coupling between Mn_1 and Mn_4 sites. At higher pressures the k_1 satellites tend to disappear together with the diffuse scattering due to the short-range order of the Tb^{3+} moments, and new peaks associated with a commensurate (C) structure with $(0,1/2,0)$ propagation vector start to appear. At 3.6 GPa and 11 K, both diffuse and incommensurate orders vanish and all intense magnetic peaks are indexed in the commensurate structure.

TABLE I. Basis function vectors for the 4*b* site, corresponding to the G_x and A_y modes of the IR Γ_3 in the *Pbnm* space group. The value of ω is $e^{i\pi k_1}$ with $k_1 = 0.27$ for incommensurate structures. The numbering of the atoms is $Mn_1(\frac{1}{2},0,0)$, $Mn_2(\frac{1}{2},0,\frac{1}{2})$, $Mn_3(0,\frac{1}{2},\frac{1}{2})$, and $Mn_4(0,\frac{1}{2},0)$. Mn_1 and Mn_4 moments are F (AF) coupled in the A_y (G_x) mode, respectively.

	Mn_1	Mn_2	Mn_3	Mn_4
G_x	(100)	(−100)	(ω00)	(−ω00)
A_y	(010)	(0 − 10)	(0 − ω00)	(0ω0)

The magnetic patterns at 3.6 GPa (Fig. 3) reflect the evolution from a commensurate structure at high temperatures (15 K and above) to the coexistence of commensurate and incommensurate structures (below 15 K). Above 15 K, only two magnetic peaks are visible, indexed as $(0,1/2,1)$ and $(1,1/2,1)$, noticing that the $l = 2n$ peaks are absent. In this temperature range, the magnetic structure was refined assuming that only the Mn moments are ordered. The best refinement corresponds to a commensurate order of the Mn moments in the A_y mode. The refined structure with $(0,1/2,0)$ propagation vector is known in manganites as the E structure. It has collinear Mn moments of equal magnitude, antiferromagnetic (AF) coupled along c and b axes, and ferromagnetic (F) coupled along a [Fig. 5(d)].

Below 15 K, the spectra become more complex. The strong increase of the intensity of the $(0,1/2,1)$ and $(1,1/2,1)$ reflections, and the onset of the $(0,1/2,0)$ and $(0,1/2,2)$ reflections [Fig. 4(c)] can be connected with the magnetic ordering of the Tb moments in a commensurate structure with the same propagation vector $(0,1/2,0)$ as that of Mn moments; the presence of $l = 2n$ reflections shows that the Tb moments order in a F mode. They likely order in a noncollinear structure, but the overlapping contributions of Tb and Mn moments and the limited number of magnetic peaks did not allow us to determine it unambiguously, so a simple Tb F-mode (F_x00) along the a axis was assumed. This assumption yields equal Tb moments of $1.8\mu_B$ at 1.5 K. More complex structures yielding inequivalent Tb moments do not change

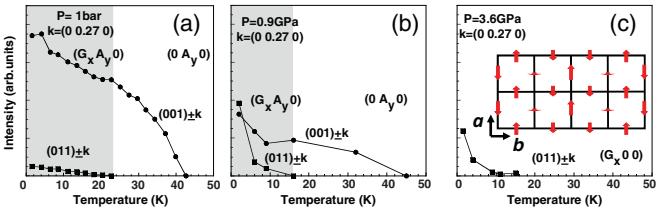

FIG. 3. (Color online) $TbMnO_3$: Temperature dependence of the integrated intensities of the k_1 satellites of the (001) and (011) reflections at $P = 1$ bar (a), 0.9 GPa (b), and 3.6 GPa (c), showing the evolution of the incommensurate structure from A_y to G_x modes with increasing pressure. Solid lines are guides to the eye. The inset in (c) shows the incommensurate G_x structure.

the results significantly. Coexisting with commensurate order, two families of incommensurate satellites, with k_1 (Mn) and k_2 (Tb) propagation vectors, are observed. Concerning Mn moments, the strong intensity of $(011)^{\pm}$ and the absence of $(001)^{\pm}$ satellites show that the incommensurate Mn structure is described by the G_x mode. As for Tb, we used the ambient pressure model to refine its contribution. The temperature dependence of the Mn and Tb moments in both commensurate and incommensurate structures is shown in Figs. 4(a) and 4(b).

To summarize, the characteristics of the pressure-induced magnetic order are as follows: (i) the onset of a commensurate magnetic order for both Tb and Mn sublattices, with an *E*-type structure for the Mn moments; (ii) a suppression of the incommensurate order in the Mn sublattice, stabilized only below ∼15 K at the highest pressure and coexisting with the commensurate order; (iii) an evolution of the incommensurate structures from A_y or (G_xA_y0) to G_x; and (iv) an increase of the magnetic length scale in the Tb sublattice which evolves

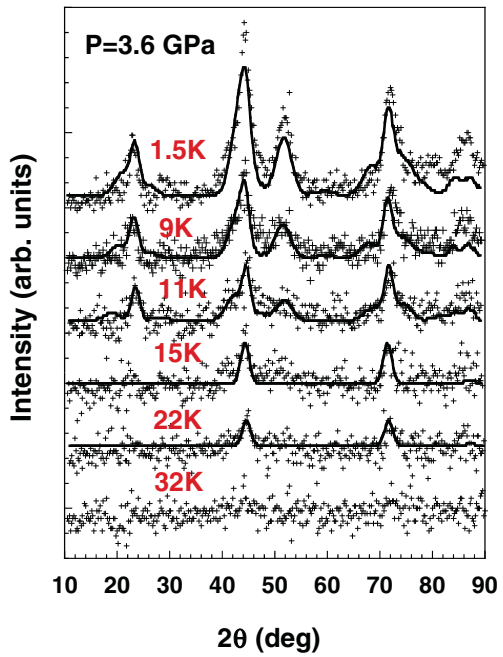

FIG. 4. (Color online) $TbMnO_3$: Temperature evolution of the magnetic diffraction patterns at 3.6 GPa. Solid lines are refinements as described in the text.

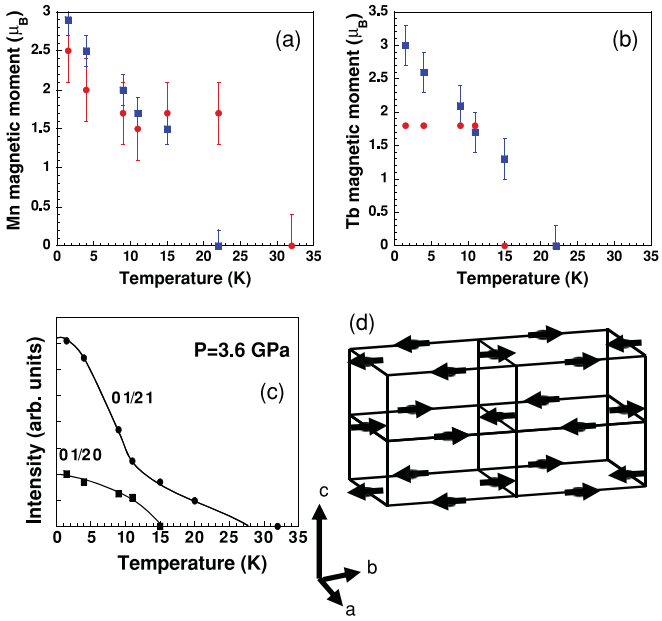

FIG. 5. (Color online) $TbMnO_3$: Temperature dependence of the magnetic moments at 3.6 GPa in incommensurate (blue squares) and commensurate (red dots) phases. (a) Mn; (b) Tb; (c) temperature dependence of the intensities of the $(0,1/2,0)$ and $(0,1/2,1)$ Bragg peaks; solid lines are guides to the eye. (d) Pressure-induced commensurate magnetic structure of *E* type (A_y mode). Only Mn moments are shown.

from short-range to long-range order. In addition, the ordering temperature of the Mn moments decreases under pressure [from 42(1) K at 1 bar to 27(5) K at 3.6 GPa], whereas that of the Tb moments increases [from 8(1) K at 1 bar to 15(3) K at 3.6 GPa].

All these features denote a change in the delicate balance of magnetic Tb-Tb, Tb-Mn, and Mn-Mn interactions which governs the phase diagram. Considering the complex interaction schemes proposed for $TbMnO_3$, still being discussed,[12–14] we cannot propose a definite explanation for the pressure effect. We can get further insight by comparing the effect of a chemical pressure, namely, of a decrease of the *R* ionic radius (where *R* is a rare earth ion) in the orthorhombic *o*-$RMnO_3$ series, to that of an applied pressure.

The magnetic phase diagram of the *o*-$RMnO_3$ family shows a decrease of T_N together with a succession of phases from *A* type to spiral-like then to *E* type, when the ionic *R* radius decreases from La to Ho.[12] Neglecting the *R* magnetism, these features are globally interpreted by a decrease of the AF Mn-Mn first-neighbor exchange interaction J_c along *c* and a change in the balance of interactions in the *ab* plane, as the the $GdFeO_3$ distortion increases.[12,13] In this plane, the super-superexchange interaction J_{2b} along *b*, involving two oxygen ions, is reinforced with respect to the F interaction J_1 between in-plane Mn first neighbors [see the Mn interaction scheme in Fig. 1(d)]. In compounds with a small radius (Tb, Y, Ho), the *E*-type structure is predicted from first-principle calculations[15] as the ground state. Experimentally, it is only observed in $HoMnO_3$ as a short-range order at low temperature,[11,16] possibly favored by the Ho moments.

$TbMnO_3$ under high pressure shows the same commensurate E structure as $HoMnO_3$ with smaller ionic radius, but here this structure is stabilized up to T_N, when the Tb moments are paramagnetic. It could therefore be directly related to the enhancement of the J_{2b}/J_1 ratio expected from theory. At lower pressures, the change in the type of incommensurate order from A_y to G_x mode suggests that the J_1 interaction also weakens with respect to the other super-superexchange interactions J_{2a} and J_3 between Mn next-nearest neighbors.[11,17]

At low temperature, the R magnetism plays an important role. The interplay between Tb and Mn orders was studied within the one-dimensional anisotropic next-nearest-neighbor Ising (ANNNI) model, considering Ising-like Tb moments, coupled by nearest- and next-nearest-neighbor interactions in a modulated Mn field.[18] A commensurate order between the Tb moments, with the same periodicity as the E structure, is found when Tb-Tb interactions are dominant. In $TbMnO_3$, the influence of Tb interactions in the energy balance increases with pressure, as shown by the opposite variations of the Néel and Tb ordering temperatures. The pressure-induced commensurate orders of both Tb and Mn moments with the same $(0,1/2,0)$ propagation vector should come from a cooperative effect of Mn-Mn, Mn-Tb, and Tb-Tb interactions.

Due to this complex energy balance, the influence of pressure on the magnetic order is much more important in $TbMnO_3$ than in $LaMnO_3$ with high ionic radius. In $LaMnO_3$ the A-type magnetic structure is a direct consequence of the orbital ordering, stabilized by AF J_c and F J_1, and low pressures have basically no effect on the magnetic order, besides an enhancement of T_N.[19] Very high pressures of the order of 20 GPa are needed to suppress the orbital order[20] and, to the best of our knowledge, their effect on the magnetic order has not been studied yet. In $TbMnO_3$, much lower pressures could tune the interplay between electronic and magnetic degrees of freedom due to the magnetic frustration.

In summary, applied pressure strongly modifies the magnetic structure of $TbMnO_3$, inducing commensurate order and changing the original incommensurate order. These changes are connected with microscopic changes of the exchange interactions. A study of the evolution of the atomic positions parameters, combined with a complete exchange scheme and/or Landau description,[21,22] could shed more light on the pressure-induced magnetic state of $TbMnO_3$, and consequently on the nature of the spin-lattice and magnetoelectric couplings.

We acknowledge support from Le Triangle de la Physique. We thank S. Petit for stimulating discussions.

*isabelle.mirebeau@cea.fr

[1] T. Kimura *et al.*, Nature (London) **426**, 55 (2003).
[2] M. Mostovoy, Phys. Rev. Lett. **96**, 067601 (2006).
[3] H. Katsura, N. Nagaosa, and A. V. Balatsky, Phys. Rev. Lett. **95**, 057205 (2005).
[4] A. Malashevich and D. Vanderbilt, Phys. Rev. Lett. **101**, 037210 (2008).
[5] D. Senff, P. Link, K. Hradil, A. Hiess, L. P. Regnault, Y. Sidis, N. Aliouane, D. N. Argyriou, and M. Braden, Phys. Rev. Lett. **98**, 137206 (2007).
[6] M. Kenzelmann, A. B. Harris, S. Jonas, C. Broholm, J. Schefer, S. B. Kim, C. L. Zhang, S. W. Cheong, O. P. Vajk, and J. W. Lynn Phys. Rev. Lett. **95**, 087206 (2005).
[7] N. Aliouane, K. Schmalzl, D. Senff, A. Maljuk, K. Prokes, M. Braden, and D. N. Argyriou, Phys. Rev. Lett. **102**, 207205 (2009).
[8] C. R. dela Cruz, B. Lorenz, Y. Y. Sun, Y. Wang, S. Park, S. W. Cheong, M. M. Gospodinov, and C. W. Chu, Phys. Rev. B **76**, 174106 (2007).
[9] I. N. Goncharenko, High Press. Res. **24**, 193 (2004).
[10] J. Rodriguez-Carvajal, Physica B **192**, 55 (1993) [http://www.ill.eu/sites/fullprof/].
[11] H. W. Brinks, J. Rodriguez-Carvajal, H. Fjellvag, A. Kjekshus, and B. C. Hauback, Phys. Rev. B **63**, 094411 (2001).
[12] T. Kimura, S. Ishihara, H. Shintani, T. Arima, K. T. Takahashi, K. Ishizaka, and Y. Tokura, Phys. Rev. B **68**, 060403(R) (2003).
[13] S. Dong, R. Yu, S. Yunoki, J. M. Liu, and E. Dagotto, Phys. Rev. B **78**, 155121 (2008).
[14] M. Mochizuki and N. Furukawa, Phys. Rev. B **80**, 134416 (2009).
[15] S. Picozzi, K. Yamauchi, G. Bihlmayer, and S. Blugel, Phys. Rev. B **74**, 094402 (2006).
[16] A. Munoz *et al.*, Inorg. Chem. **40**, 1020 (2001).
[17] F. Quezel, J. Rossat-Mignod, and E. F. Bertaut, Solid State Commun. **14**, 941 (1974).
[18] O. Prokhnenko, R. Feyerherm, M. Mostovoy, N. Aliouane, E. Dudzik, A. U. B. Wolter, A. Maljuk, and D. N. Argyriou, Phys. Rev. Lett. **99**, 177206 (2007).
[19] L. Pinsard-Gaudart, J. Rodriguez-Carvajal, A. Daoud-Aladine, I. Goncharenko, M. Medarde, R. I. Smith, and A. Revcolevschi, Phys. Rev. B **64**, 064426 (2001).
[20] I. Loa, P. Adler, A. Grzechnik, K. Syassen, U. Schwarz, M. Hanfland, G. K. Rozenberg, P. Gorodetsky, and M. P. Pasternak, Phys. Rev. Lett. **87**, 125501 (2001).
[21] P. Toledano, Phys. Rev. B **79**, 094416 (2009).
[22] J. L. Ribeiro and L. G. Ribeira, Phys. Rev. B **82**, 064410 (2010).